

Increasing the operational and environmental performance of a diesel power installation by utilizing water-based fuel

Al-Maidi A. A. H^{1*}, B.T.Sh. AL-Mosawi², Hayder Al-Lami³, Rodionov Yu. V.^{4,5}, Lomovskikh A. E.⁵, Sever A. V.⁵, Rybin G. V.⁴, Mohammed Sabeeh Majeed⁶, Ahmed Kateb Jumaah Al-Nussairi⁷

¹Plant Protection Dept, Coll. of Agriculture, University of Misan, Misan, Iraq; ali_abbas@uomisan.edu.iq (A.M.A.A.H.).

²University of Misan College of Education; buraq@uomisan.edu.iq (B.T.S.A.M.)

³University of Misan, College of engineering, Iraq; hayderallami@uomisan.edu.iq (H.A.L.)

⁴FGBOU VO "Tambov State Technical University"; rodionow.u.w@rambler.ru (R.Y.V.)

⁵Federal State Budgetary Educational Institution of Higher Education Michurinsk State Agrarian University; lomovskikh1979@yandex.ru (L.A.E.) enot1237@gmail.com (S.A.V.)

⁶Al-Manara College for Medical Sciences; mohammedsabeeh@uomanara.edu.iq (M.S.M.).

⁷University of Manara; ahmedkateb@uomanara.edu.iq (A.K.J.A.N.)

Abstract: A new device for enhancing the physicochemical properties of diesel fuel to improve the combustion process and the operational and environmental performance of diesel power plants (DPP) of agricultural machinery (AM). During regular operation, DPP indicators are decreased due to various factors including the formation of carbon deposits on the surfaces of parts, causing AM to no longer meet efficiency and environmental standards. The conducted analysis of the AM operation showed that the thermal stress of the parts is increased as a result of forming carbon deposits in the combustion chamber of the DPP. To address this issue, the proposal is to utilize a technical liquid (water) that will be directed to the combustion chamber of the DPP. This process will effectively clean the surface of the carbon deposits and prevent their future formation through the microwave action of the steam-air mixture prepared in the intake manifold. For this purpose, a device has been developed to be installed on board the SHT, integrated into the standard fuel system, allowing the preparation of watered diesel fuel. As a result of complex dynamic processing, a highly dispersed emulsion is prepared from diesel fuel and water, the combustion of which in the combustion chamber of the DSU allows for the complete removal of the formed carbon deposit. The findings show that utilizing the developed device will improve the operational and environmental performance of the DSU, increase the capacity of old equipment by up to 15%, reduce specific fuel consumption by up to 18%, and the soot content in the exhaust gases by up to 14%.

Keywords: Agricultural machinery, Carbon deposits, Diesel power plant, Operational and environmental performance.

1. Introduction

The development of the agro-industrial complex (AIC) directly depends on the state of the agricultural enterprises (AE) that are part of it. The technical readiness of the machine and tractor fleet (MTF) used at each enterprise affects the level of AE development. The level of development directly depends on the technical readiness of each element of agricultural machinery (AE), which is part of the MTF system. Consequently, the level of operability of each mechanism, unit and part determines the technical readiness of AE. It is worth noting that the most important unit of AE is the diesel power plant (DPP), which includes complex mechanisms and parts [18].

During the daily operation of DPP, they are exposed to many factors (low quality of fuel and oils, constantly changing operating modes, oxidation of lubricating oil and many others). These factors ultimately lead to the formation of carbon deposits and deposits on the surface of pistons and other parts. Moreover, it leads to the deterioration of fuel combustion and an increase in the compression

ratio, which increases the average rate of pressure and leads to “rigidity” of the DEU operation and, most importantly, a decrease in their operational and environmental performance [19].

Carbon deposits are products of incomplete combustion of fuel. Carbon deposits are also a good heat insulator, the formation of which on the parts of the cylinder-piston group (CPG) and the gas distribution mechanism (GRM) leads to a disruption of heat exchange and redistribution of heat flows. The resulting decrease in piston temperature and increase in the temperature of the CPG liner contributes to an increase in the thermal gap between the piston and the liner, resulting in a decrease in compression. As a result, the performance of the DEU deteriorates, power decreases and fuel consumption increases in all operating modes of the DEU, which will be especially evident in the SHT with high mileage and service life [20].

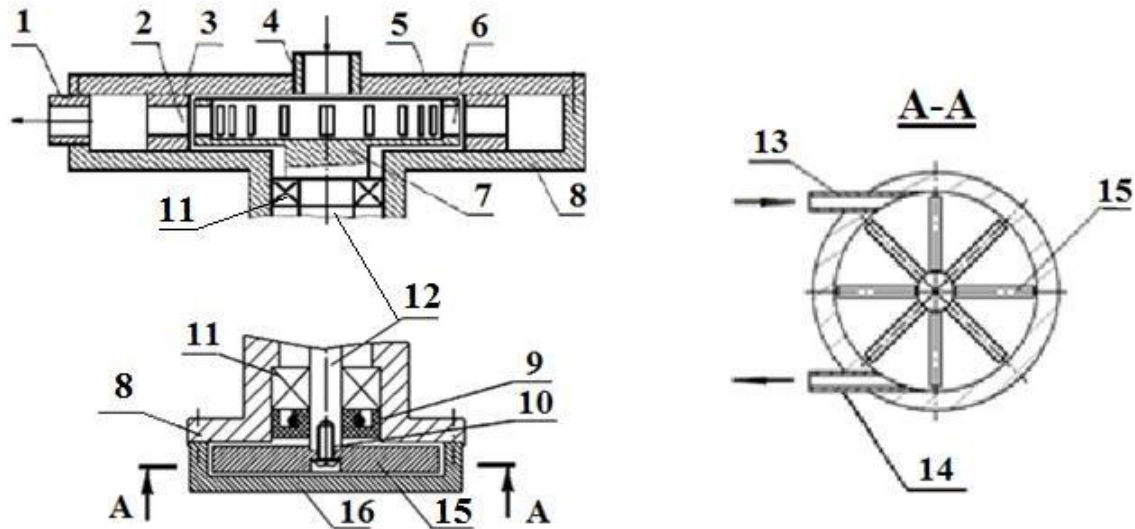
Studies [1] have established that with a carbon deposit thickness of about 3 mm on the parts of the crankshaft and gas distribution mechanism, an increase in pressure at the end of the compression stroke by 8...10% is observed, which leads to an increase in the "rigidity" of the fuel combustion process (more than 0.25...0.30 MPa) per 10 of the crankshaft rotation angle, as a result of which the effective power of the DEU decreases by 5-6%, and the specific fuel consumption increases by 3-4% compared to the nominal values [2]. This is also explained by an increase in mechanical losses due to an increase in the maximum cycle pressure by 16% and an average rate of pressure increase in the cylinder of up to 22%. The thickness of the carbon deposit only increases over time, therefore, the above indicators will only worsen. Cleaning DEU parts from carbon deposits is a complex and labor-intensive process and it is not included in the list of works on technical maintenance of the SHT [3]. Thus, when the DEU has been in operation for more than 2600 engine hours, the carbon deposits on the piston vary within the range of 1 to 2 mm and significantly reduce the operational and environmental performance of the DEU of the currently used SHT models. In this regard, in order to improve these performance indicators of the DEU, it is proposed to use watered diesel fuel (WDF), the preparation of which is advisable to carry out directly on the equipment using a device developed for these purposes [4].

Water added to the combustion chamber during the intake and compression strokes (at temperatures up to 500 °C) will initially sharply overheat into droplets of steam, which will move chaotically and collide with the carbon deposit surface. With a further increase in temperature (over 1000 °C) during the power stroke (combustion), the steam particles will "micro-explode", which, when exposed to the carbon deposit surface, will lead to the chipping off of its micro-particles. This is the process of microwave action of the steam-air mixture with the carbon deposit surface in the combustion chamber of the DEU, leading to its gradual removal due to the resulting "micro-explosions" of steam particles [5].

2. Materials and Working Methods

Thus, to solve the problem, it is necessary to analyze the methods and means for preparing ODT.

Currently, various mechanical devices are used to prepare water-fuel emulsions. Such devices are built into the standard fuel system and process the entire volume of fuel that passes through it. At the same time, the physical and chemical properties of the fuel are improved based on cavitation treatment formed when passing through the device. The analysis of these devices allowed us to identify the most promising designs [6, 7], which were taken as a prototype of the developed more efficient device. The basic diagram and main design elements of such a device are shown in Figures 1, 2.



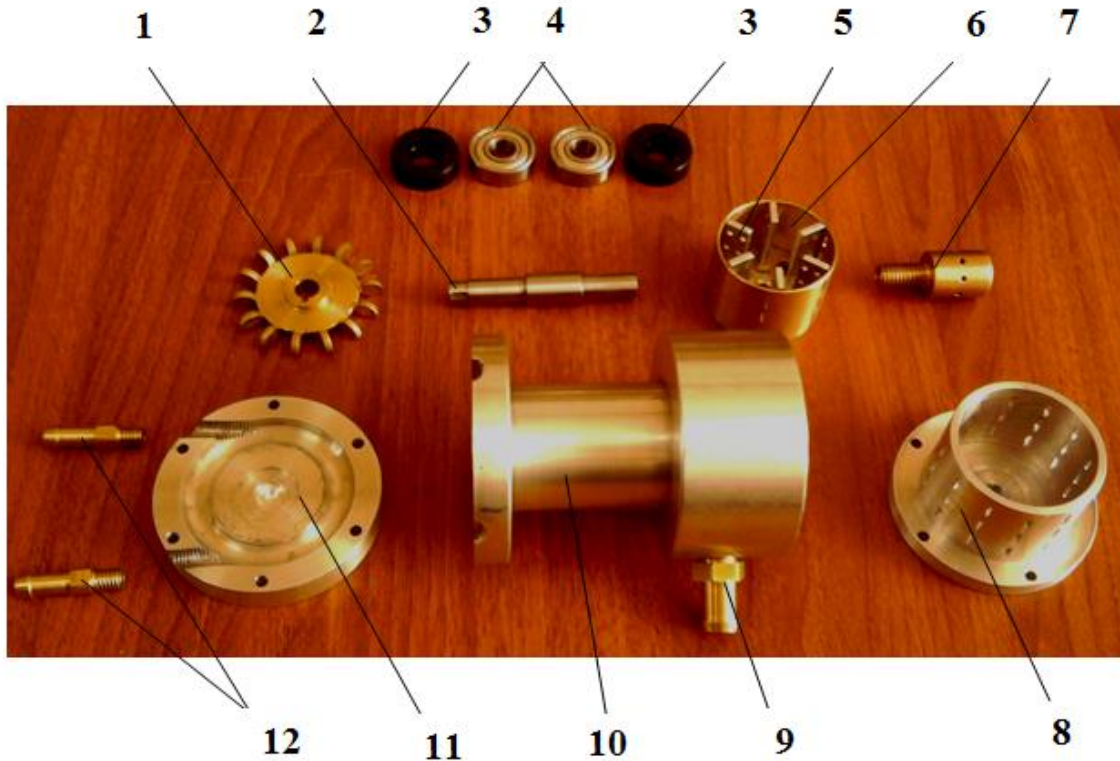
1 – outlet pipe; 2 – internal channels; 3 – sound camera; 4 – supply fitting; 5 – front cover; 6 – slot channels in the rotor; 7 – rotor; 8 – body; 9 – oil seal; 10 – screw; 11 – bearing; 12 – rotor shaft; 13 – inlet fitting; 14 – outlet fitting; 15 – impeller; 16 – rear cover

Figure 1.

Rotary-pulsation apparatus for the preparation of ODT.

The device (rotary-pulsation apparatus) is improved by installing: at the inlet of the apparatus of the dispenser-cavitator; on the rotor shaft of a rigidly mounted blade impeller; on the cover of the device of the inlet and outlet pipes, the longitudinal axes of which are located in the plane passing through the end of the blade impeller in its middle part, while the inlet pipe is connected to the external pump, and the outlet pipe is connected to the inlet pipe of the apparatus. The proposed design ensures the mixing of two mutually insoluble liquids (diesel fuel and water), which improves the dispersion and homogenization of the prepared mixture with the minimum diameter of the crushed droplets of the aqueous phase of no more than $2 \mu\text{m}$.

The model of the developed rotary-pulsation apparatus (RPA) was made in the automated design system SolidWorks-2016 and Nero-2012. Based on the received drawings, the developed apparatus was manufactured, the details of which are shown in Figure 2.



1 - impeller; 2 - drive shaft; 3 - seal; 4 - bearing; 5 - rotor impeller; 6 - rotor; 7 - additional cavitator; 8 - stator; 9 - outlet nozzle; 10 - housing; 11 - cover; 12 - nozzles

Figure 2.

RPA parts manufactured according to the developed drawings.

The rotary-pulsation device consists of working bodies made in the form of a rotor 16 and a stator 2, located in housing 1, the rotor is rigidly fixed with a screw 10 to the shaft 13 and rotates on two bearings 8. The bladed impeller 21 is rigidly mounted on the rotor shaft 13 using a screw 15 and is designed to drive the rotor shaft by using a liquid jet, which is supplied under pressure by an external pump. On cover 20 of housing 1, the inlet 9 and outlet pipes 17 are installed, the longitudinal axes of which are located in the plane passing through the end of the impeller blade in its middle part, wherein the inlet pipe is connected to the pump, and the outlet pipe is connected to the inlet pipe of the device. The inlet pipe 9 is intended for supplying the processed liquid components to the impeller blades, and the outlet pipe 17 is intended for removing the processed liquid components from the impeller blade. The inner space of the housing 1 is sealed with a gland 6. The housing 1 is a cylindrical cavity and has an outlet pipe 11 and an inlet pipe 12. The rotor 16 is made in the form of a disk, on the working surface of which there are inlet blades 3 of the pump, the outlet blades 5 of the pump are arranged in rows along concentric circles, consisting of protrusions and depressions. The inlet blades 3 of the pump are made together with the rotor and have a flat rectangular shape, their number should be no less than the number of depressions on the rotor. The inlet blades 3 of the pump are intended for feeding the VDS components to the toothed elements 4 of the stator and 5 of the rotors. The stator 2 is made in the form of a disk, on the working surface of which toothed elements 5 are made, which are outlet blades located in rows along concentric circles and consisting of projections and depressions, wherein each row of the toothed element 4 of the stator 2 is covered by a row of the toothed element 5 and are also made in three rows and in two stages. The outlet blades 5 of the pump are necessary for moving the processed VDS from the toothed elements 5 of the rotor 16 and the stator 2 to the outlet pipe 11, and the greater the thickness of the outlet blade 5 of the pump, the greater the pressure. The toothed elements 5 of the rotor

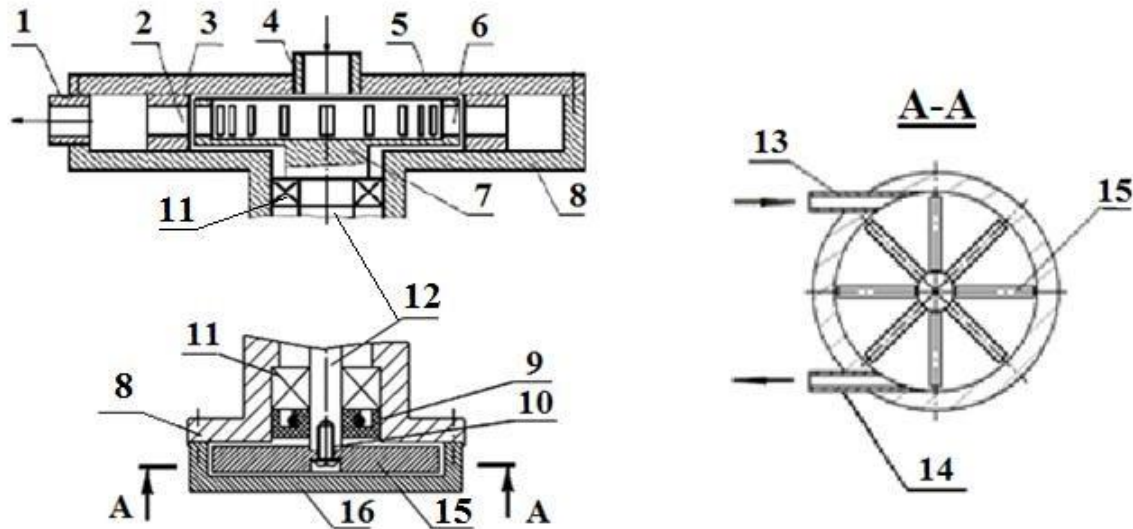
19 to a liquid tank 2. The water tank has a jacket that is connected to the DEU exhaust system 23, as a result of which the water is heated, which ensures uninterrupted operation of the system during the winter period of operation. At the end of the dispenser, there is a vacuum chamber 13, regulating the water supply depending on the load on the DEU and connected through a vacuum tube 12 to the intake manifold 11 of the DEU. The dispenser 5 is a jet-cavitation ejector, which is connected via a fuel hose 10 to a mixing tank 3, which has a shut-off needle 14 with a float 15 for adjusting the level of the ODT. Then the ODT of coarse dispersion is taken from the mixing tank 3 by the second additional fuel pump 6 and fed to the RPA 8. The rotary-pulsation apparatus is driven into rotation by the stream of passing fuel and has a fixed shaft rotation frequency, then the resulting ODT is fed back to the mixing tank 3. Thus, there is a constant mixing of the ODT located in mixing tank 3, in which a stable and highly dispersed ODT is formed. Mixing tank 3 has a liquid jacket that is connected to the cooling system of the DEU 9, as a result of which the ODT in mixing tank 3 is heated to the required temperature (50...60 °C). Then the prepared ODT is taken by the standard fuel pump 18 and fed through the fuel hose 10 to the power supply system of the DEU 9. The control unit 21, depending on the operating temperature of the DEU, controls the liquid valve 19 and the second additional fuel pump 6, depending on the ODT processing time, turns them on and off.

The complex of these devices operates as follows.

1. When starting the DEU, fuel from fuel tank 1 through the fuel line 10 is taken by the first additional pump 4 and fed through the dispenser 5, the liquid valve 19 into the mixing tank 3. Together with the fuel, a metered amount of water is taken. Then the standard fuel pump 18 takes fuel through the intake pipe and feeds it to the DEU 9.

2. When the DEU warms up to the operating temperature, control unit 21 receives information from the temperature sensor and opens valve 19 and the second additional fuel pump 6 is switched on, while the first additional pump 4 supplies fuel under pressure to the dispenser 5. The vacuum in the intake manifold of the DEU 11 is transmitted to the vacuum chamber 13 of the dispenser 5, which regulates the supply of water taken by the fuel stream passing under pressure. Then, the coarse-dispersed ODT obtained in dispenser 5 enters mixing tank 3, in which, as it is filled with the mixture, float 15 floats up and, acting on the shut-off needle 14, shuts off the supply of ODT to the tank 3, thereby ensuring a constant level. At this point, the first additional pump 4 is automatically switched off. Then, from mixing tank 3, the ODT is taken by the second additional fuel pump 6 and fed to RPA 8, where the water in the diesel fuel is crushed, and mixed, and the resulting finely dispersed ODT is fed back to the mixing tank 3. After that, the ODT is taken from the mixing tank 3 by the standard fuel pump 18, through the fuel hose 10 and fed to the DEU 9.

3. When the DEU is stopped when the ODT is used without an emulsifier, then during the stratification of water from the ODT in the mixing tank 3, a mixture of water and heavy hydrocarbons accumulates at the bottom of the tank 3, which is mixed in the ODT during the next start. The basic diagram of the developed RPA is shown in Figure 4.



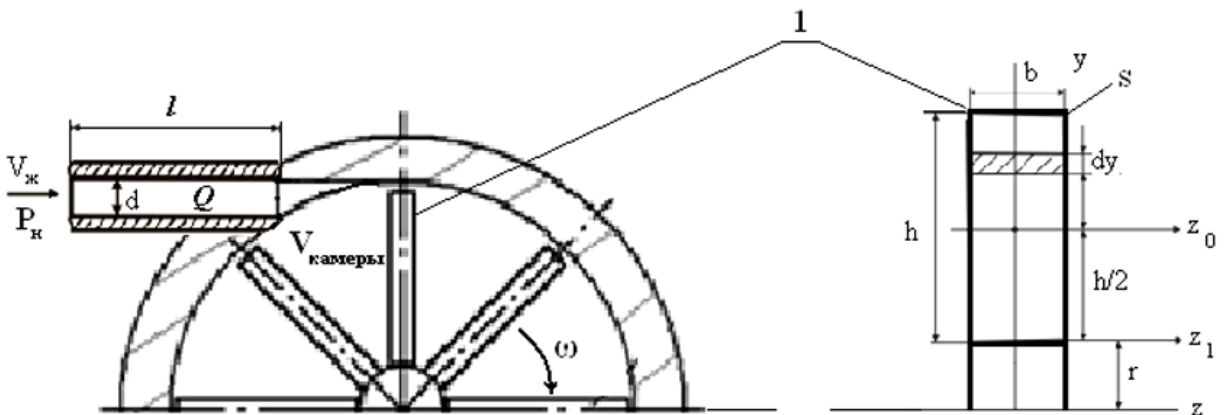
1 - outlet pipe; 2 - internal channels; 3 - sound chamber; 4 - feed nozzle; 5 - front cover; 6 - slotted channels in the rotor; 7 - rotor; 8 - housing; 9 - gland; 10 - screw; 11 - bearing; 12 - rotor shaft; 13 - inlet nozzle; 14 - outlet nozzle; 15 - impeller; 16 - rear cover

Figure 4.

Schematic diagram of the developed device.

Since this device is proposed to be used directly on board the SHT, then to reduce the costs spent on its drive, a device design with a drive from the stream of the processed liquid is proposed, so as not to use an electric drive. Therefore, an additional section with an impeller 15 is installed in the design of the device, which allows for the drive from the stream of passing liquid. In this case, the rotor speed will depend on the pressure of the stream created by the feed pump.

The schematic diagram of the device's drive design is shown in Figure 5.



1 – impeller blade; V_l – fluid velocity (fuel emulsion); P_H – supply pump pressure; d – internal diameter of the inlet pipe; l is the length of the inlet pipe; Q – fluid flow through the inlet pipe; $V_{chambery}$ – the volume of one impeller chamber; ω – angular speed of the impeller; b – width of the impeller blade; h – height of the impeller blade; r – radius of the impeller hub (disk); s – impeller blade thickness

Figure 5.

The schematic diagram of the device's drive design.

The rotor drive of the device is a hydraulic turbine, in which the working element (a wheel with blades or an impeller) receives energy from the liquid coming from the pump into the inlet branch pipe 5

and converts it into mechanical energy of rotation of the shaft of the device. The task of calculating the rotor drive is to determine the dependence of the impeller speed (n) on the dimensions of the wheel with blades (a, b, h, s, r), the internal diameter (d) and length (l) of the inlet branch pipe and the pressure of the feed pump (P_n). The resulting mathematical relationship allows us to determine the overall dimensions of the impeller to ensure the required rotation frequency of the rotor of the device.

The rotor impeller receives kinetic energy from the liquid entering the inlet pipe from the pump and converts it into mechanical energy of rotation of the device drive shaft. The liquid, under the influence of pressure H , is supplied at high speed to the nozzle nozzle in the form of a jet, which then hits the impeller blades, giving the rotor additional rotation. The speed will be determined by the formula [8,9,10]:

$$V_c = \varphi \sqrt{2gH}, \quad (1)$$

Where φ – speed coefficient for the nozzle equal to 0.98...0.99.

At the angular speed of rotation of the impeller ω power N , the power transferred by the liquid through the blades of the impeller to the shaft, equal to

$$N = M\omega. \quad (2)$$

Moment of external force M on the rotor shaft is determined as the product of this force F to the shaft radius r_g , so that $M\omega = F\omega r_g$, $\omega r_g = u_g$ – peripheral speed on the shaft. After transformation we get the expression:

$$N = Fu_g. \quad (3)$$

In order to improve the functioning of this device, it is necessary that the passing stream of the liquid component transfer its energy directly to the drive impeller as efficiently as possible. This is possible when the speed V_c the jet at the outlet of the apparatus will become equal to or approach the speed of the drive impeller, i.e. $V_c = u_g$.

The force of interaction between a liquid jet and a flat impeller blade will be determined by the expression [11]:

$$F = 2\rho g S \frac{V_c^2}{2g} = 2\gamma S \frac{V_c^2}{2g}. \quad (4)$$

where ρ – is the density of the liquid, kg/m³; g – gravity acceleration, m/sec²; γ – specific gravity of liquid, N/m³, $\gamma = \rho g$; S – jet cross-sectional area, m².

Let us accept $H = \frac{V_c^2}{2g}$, then the impact force can be expressed in terms of pressure and hydrostatic pressure p :

$$F = 2\gamma HS = 2pS. \quad (5)$$

Then the power developed by the impeller will be equal to:

$$N = Fu_g = 2pSu_g = 2pSV_c = 2pS\omega r_g. \quad (6)$$

On the other hand, the power of the impeller can be expressed in terms of the kinetic energy of impeller E_{kp} per unit of time t [12]:

$$N = \frac{E_{kp}}{t} = \frac{J_{kp} \omega^2}{2t}, \quad (7)$$

Where J – moment of inertia of the impeller, kg m^2 ; ω – angular speed of rotation of the impeller, s^{-1} . The moment of inertia of the impeller is the sum of the moment of inertia of the impeller disk J_o and moment of inertia of the blades J_n quantity N :

$$J_{kp} = J_o + NJ_n. \quad (8)$$

Moment of inertia J_o impeller disk radius r corresponds to [13]:

$$J_o = m_1 r^2, \quad (9)$$

Where m_1 – disk weight, kg ; $m_1 = \rho \pi r^2 b$. Then we get :

$$J_o = m_1 r^2 = \rho \pi r^2 b r^2 = \rho \pi r^4 b. \quad (10)$$

The impeller blade has a rectangular shape (Figure 2), then the moment of inertia of a rectangle with base b and height h relative to the central axis is determined [14]:

$$J_{np} = \int_{-\frac{h}{2}}^{\frac{h}{2}} y^2 b dy = \frac{bh^3}{12}. \quad (11)$$

Moment of inertia of the impeller blade relative to the central axis Z determined by Steiner's theorem [15]:

$$J_{npz} = \left[\sqrt{\frac{bh^3}{12}} + \left(\frac{h}{2}\right)^2 \right] \cdot m_2, \quad (12)$$

Where m_2 – weight of the impeller blade, kg ; $m_2 = \rho h b s_1$.

Then the moment of inertia of the impeller blade is determined:

$$J_n = J_{npz} = \left[\sqrt{\frac{bh^3}{12}} + \left(\frac{h}{2}\right)^2 \right] \rho h b s_1. \quad (13)$$

Substituting expressions (10) and (13) into expression (8), we determine the moment of inertia of the impeller:

$$J_{kp} = J_o + NJ_n = \rho \pi r^4 b + N \left[\sqrt{\frac{bh^3}{12}} + \left(\frac{h}{2}\right)^2 \right] \rho h b s_1 = \rho b \left[\pi r^4 + N h s_1 \left(\sqrt{\frac{bh^3}{12}} + \left(\frac{h}{2}\right)^2 \right) \right]. \quad (14)$$

Then the kinetic energy of the impeller will be:

$$E_{kp} = \frac{J_{kp} \omega^2}{2} = \frac{\omega^2 \rho b}{2} \left[\pi r^4 + N h s_1 \left(\sqrt{\frac{bh^3}{12}} + \left(\frac{h}{2}\right)^2 \right) \right]. \quad (15)$$

We substitute expression (15) into (7) and equate it with expression (6):

$$2pS\omega_g = \frac{\omega^2 \rho b}{2t} \left[\pi r^4 + N h s_1 \left(\sqrt{\frac{bh^3}{12}} + \left(\frac{h}{2}\right)^2 \right) \right].$$

or

$$tpSr_g = \omega \rho b \left[\pi r^4 + Nhs_1 \left(\sqrt{\frac{bh^3}{12} + \frac{h^2}{4}} \right) \right]. \quad (16)$$

We determine the angular speed of rotation of the impeller:

$$\omega = \frac{pSr_g t}{\rho b \left[\pi r^4 + Nhs_1 \left(\sqrt{\frac{bh^3}{12} + \frac{h^2}{4}} \right) \right]}, \quad (17)$$

where p – the fluid pressure in the inlet pipe, N/m²; S – cross-sectional area of the jet, m², $S = \frac{\pi d^2}{4}$; d – diameter of the inlet pipe, m; r_g – radius of the impeller shaft, m; ρ – liquid density, kg/m³; b – impeller width, m; r – radius of the impeller hub, m; N – number of impeller blades, pcs.; h – height of the impeller blade, m; S_1 – thickness of the impeller blade, m.

Assuming that $\omega = \frac{\pi n}{30}$, sec⁻¹

and $n = \frac{30\omega}{\pi}$, rpm, you can write the expression:

$$n = \frac{30pSr_g t}{\pi \rho b \left[\pi r^4 + Nhs_1 \left(\sqrt{\frac{bh^3}{12} + \frac{h^2}{4}} \right) \right]} = \frac{7,5pd^2 r_g t}{\rho b \left[\pi r^4 + Nhs_1 \left(\sqrt{\frac{bh^3}{12} + \frac{h^2}{4}} \right) \right]}. \quad (18)$$

The resulting mathematical relationship shows that the number of revolutions of the impeller (rotor shaft) is directly proportional to the fluid pressure in the inlet pipe, the diameter of the inlet pipe, the radius of the impeller shaft and inversely proportional to the density of the impeller material and its geometric dimensions.

Then, by carrying out appropriate calculations, the main structural dimensions of the device were determined, after which it was manufactured in metal. The proposed design does not require large material costs for manufacturing, since standard industrially manufactured parts are used.

After that, a detailed study was carried out of the working process of a 4-stroke diesel power plant (YaMZ-236D-3) when operating on an ODT prepared by the developed device, in a wide range of load conditions.

For this purpose, the developed device was built into the standard power supply system of the diesel engine according to the diagram presented in Figure 6.

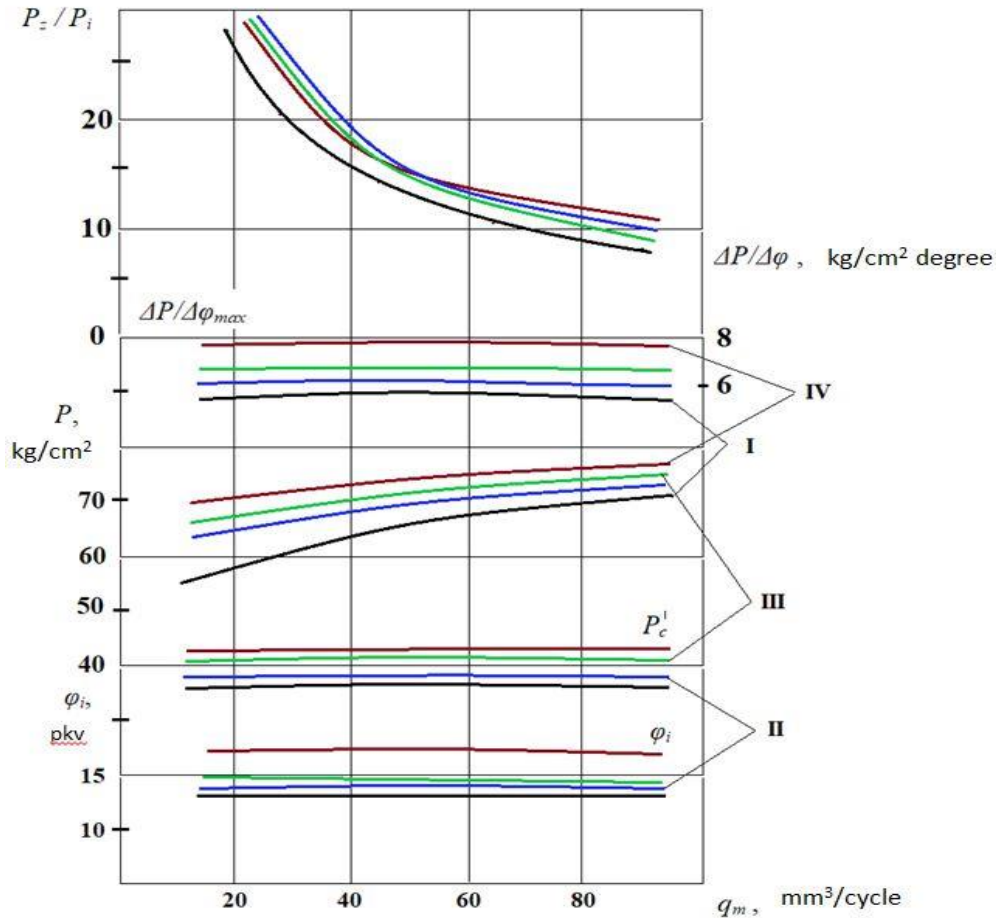


Figure 6.
External appearance of the experimental setup.

To conduct the research, the developed device was built into the standard power supply system of the DEU, according to the diagram in Figure 3. At the same time, in order not to worsen the operational and environmental performance of the DEU, it is proposed to supply water to diesel fuel no more than 5% of the fuel consumption. The experimental setup is a KI-5540 load stand with a diesel power plant (YaMZ-236D-3) installed on it. In addition to standard measuring instruments, this setup allows for the removal of indicator diagrams and recording of fuel pressure in front of the nozzle, needle lift of the nozzles, exhaust gas smoke, etc. The study was conducted at the most typical operating speed modes ($n = 1000 \dots 1900 \text{ min}^{-1}$) and in the entire range of load changes. The determining factor in the operation of the DEU at partial loads is a decrease in the supply of ODT with an almost unchanged amount of air charge.

In this regard, the main feature of the working process of the DEU (YaMZ-236D-3) when working on the ODT, in this case, is a significant total excess of air during combustion. At idle speed of the DEU, the excess air coefficient can reach ($\alpha = 0.8 \dots 1.0$). The second feature is a decrease in the amount of heat released, in connection with this, a decrease in the temperature of the engine parts due to the high heat capacity of the water contained in the ODT, which takes part of the heat from the heated parts of the DEU for its own heating. Reducing the load significantly affects the process of filling the cylinders, an insignificant increase in the filling coefficient is due to a decrease in air heating at the inlet to the DEU. There is also an insignificant effect of the load on the compression process, the main effect is exerted by an increase in the excess air coefficient (α), which is determined during the combustion process [16].

Figure 7 shows graphs illustrating the dependence of the main indicators of the working process of the DEU (YaMZ-236D-3) on the amount of ODT supply (with a water content of up to 5%).



I – at $n = 1000 \text{ min}^{-1}$; II – at $n = 1350 \text{ min}^{-1}$;
 III – at $n = 1650 \text{ min}^{-1}$; IV – at $n = 1950 \text{ min}^{-1}$

Figure 7.

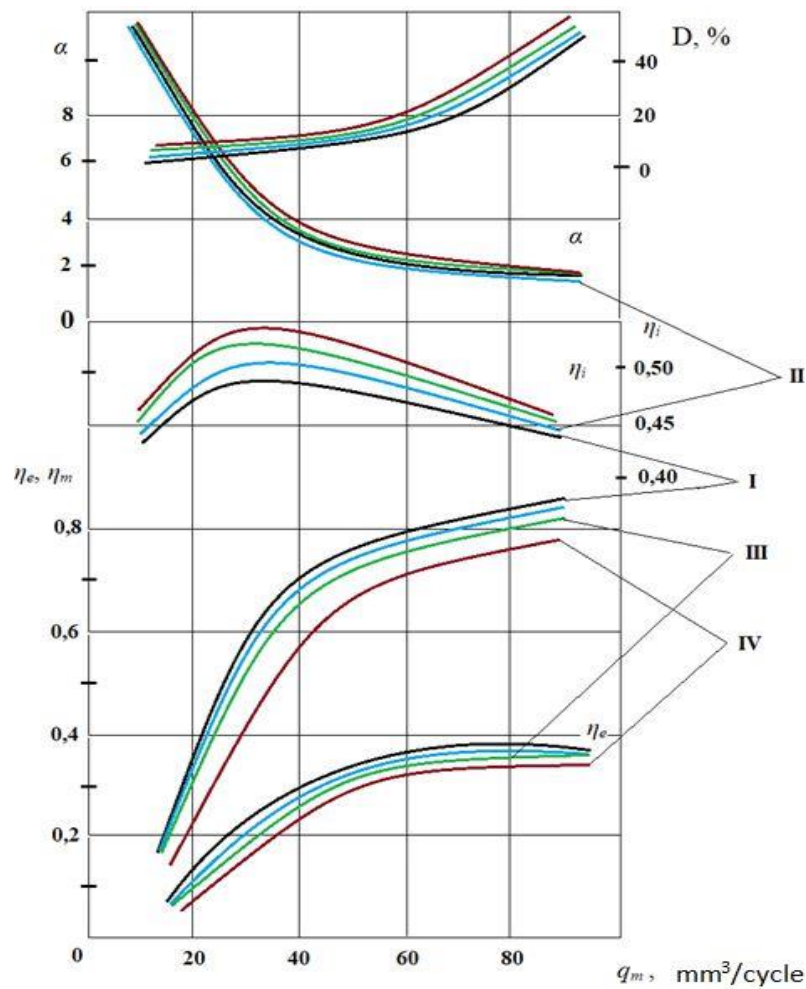
Dependence of the operating process indicators of the DEU (YaMZ-236D-3) when operating on the ODT.

As follows from these graphs, presented in Figure 7, the ignition delay of the ODT weakly depends on the load, although there is a tendency for the fuel injection advance angle (φ_i) to increase with a decrease in the ODT supply. The duration of the period of a sharp increase in pressure with a decrease in load is reduced, and the maximum flash pressure P_z and the “rigidity” of the combustion process ($\Delta P/\Delta\varphi_{max}$) do not decrease significantly.

Thus, at $n = 1300 \dots 1900 \text{ min}^{-1}$, a significant decrease in load causes a decrease in P_z by only 4...5 kg/cm^2 , and the “rigidity” of the combustion process ($\Delta P/\Delta\varphi_{max}$) does not change significantly when the DEU is operating on the ODT. The ratio P_z / P_i increases significantly.

Thus, with a decrease in load, the mechanical stress of the DEU parts (YaMZ-236D-3) practically does not decrease. Even at low loads, the DEU on the ODT operates under conditions where the flash pressure and the “rigidity” of the combustion process are almost equivalent to the pressure and rigidity in the maximum load mode.

Figure 8 shows the dependence of the indicated (η_i), effective (η_e) and mechanical (η_m) efficiency, excess air coefficient (α) and exhaust smoke (D , %) of the DEU (YaMZ-236D-3) on the ODT feed value. The economic qualities of the working process occurring in the combustion chamber of the DEU (YaMZ-236D-3) decrease with a decrease in the supply of ODT (with a water content of up to 5%).



I – at $n = 1000 \text{ min}^{-1}$; II – at $n = 1350 \text{ min}^{-1}$;
 III – at $n = 1650 \text{ min}^{-1}$; IV – at $n = 1950 \text{ min}^{-1}$

Figure 8.

Dependence of indicator (η_i), effective (η_e) and mechanical (η_m) efficiency, excess air coefficient (α) and exhaust gas opacity (D , %) of a diesel engine (YaMZ-236D-3) on the amount of ODT supply.

From the graph in Figure 5 it is clear that the indicator (η_i) efficiency factor (efficiency) increases when q_t is reduced to $35...40 \text{ mm}^3/\text{cycle}$. With a further decrease in the ODT supply, which practically corresponds to the idle speed of a diesel engine, η_i decreases significantly. An increase in η_i with a decrease in load ensures fairly high values of the effective efficiency - η_e , as well as its flat change, despite the decrease in mechanical efficiency - η_t . This is a positive feature of the operation of a diesel engine (YaMZ-236D-3) on the ODT at partial loads. An increase in η_i with increasing α is possible due to a reduction in the combustion time of ODT due to the addition of water to the combustion zone [17].

To confirm this issue, it is advisable to consider the balance of heat losses, in which the theoretical efficiency - (η_T) is calculated for a cycle with heat supply $V = \text{const}$ and with a variable heat capacity. The heat loss balance takes into account work losses due to various reasons.

$$Q_p = q_{deg} + q_{oxl} + q_{np\theta}, \quad (19)$$

where q_{tp} – loss of useful work in the cylinder; q_{deg} – losses of useful work associated with imperfections in the dynamics of the combustion process; q_{oxl} – loss of useful work due to heat transfer and non-burnout of emulsified fuel; q_{prv} – losses of useful work associated with losses in output.

These losses, expressed in kJ , related to the total amount of heat introduced into the cycle are graphically presented in Figure 6.

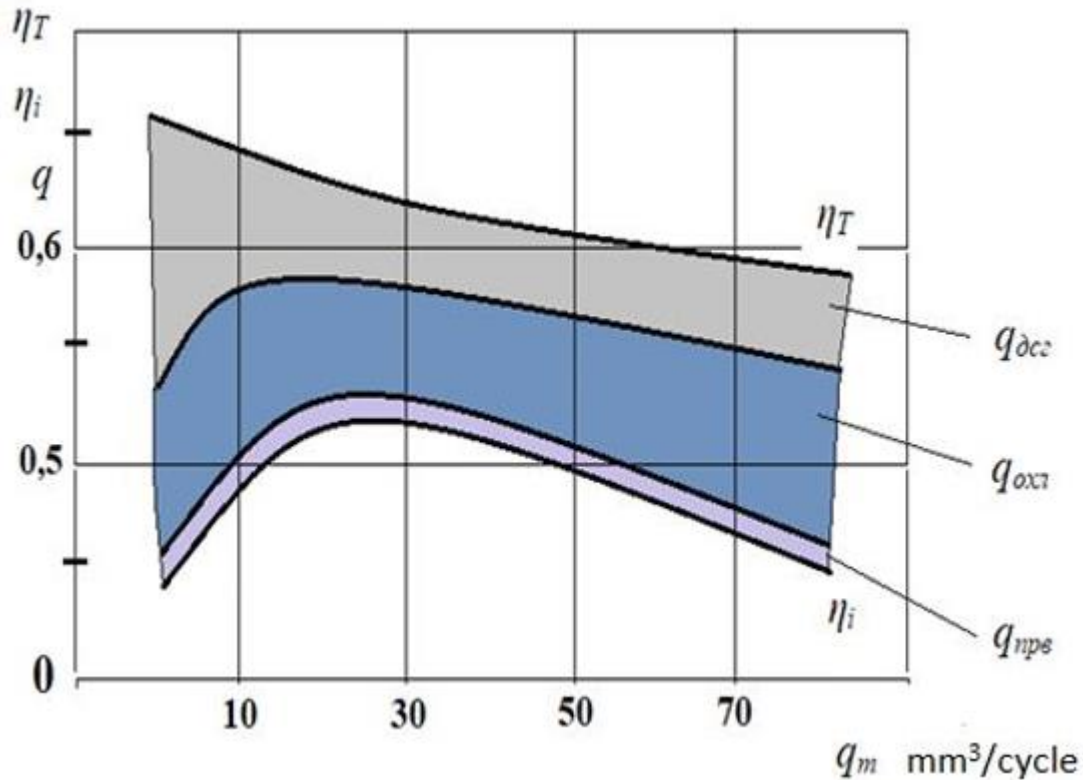


Figure 9.
Graphical dependence of the loss balance for different ODT supply at $n = 1500 \text{ min}^{-1}$.

Analysis of the graph presented in Figure 6 allows us to establish that the main reason for the increase in indicator efficiency (η_i) with a decrease in the supply of ODT is the increase in the efficiency of the theoretical cycle (η_T) determined by the decrease in the heat capacity of the working fluid due to a drop in the cycle temperature (due to the addition of air mixture of water) and saturation of combustion products with diatomic gas (CO_2).

It is also clear from the graph in Figure 6 that the reason for the drop in η_i when supplying ODT is less than $30 \text{ mm}^3/\text{cycle}$ is a sharp deterioration in the combustion process of such fuel.

A reduction in combustion duration, expressed in a decrease in q_{dsg} , is also observed when the load is reduced to certain limits and is the second reason for the increase in indicator efficiency (η_i), but its quantitative effect on η_i is estimated on average at 1...2%. The third reason for the increase in η_i is the increase in the completeness of combustion of the ODT due to the addition of a small amount of water (less than 5%), as evidenced by a decrease in the opacity of exhaust gases with a decrease in fuel supply [13].

The obtained smoke measurement values of the DEU (YaMZ-236D-3) are presented in Table 1.

Table 1.
Results of smoke measurement of DEU (YaMZ-236D-3).

№ tests	Results of the obtained values			
	Measurements obtained when operating a diesel engine using conventional diesel fuel		Measurements obtained during the operation of the Daewoo on the ODT	
	$K(M^{-1})$	$N(\%)$	$K(M^{-1})$	$N(\%)$
1	4,03	74,69	3,93	73,63
2	3,94	75,58	3,36	74,37
3	3,89	81,42	3,78	80,37
4	4,01	75,64	3,89	73,9
5	3,97	75,87	3,71	74,53
Average value	3,968	76,64	3,734	75,36

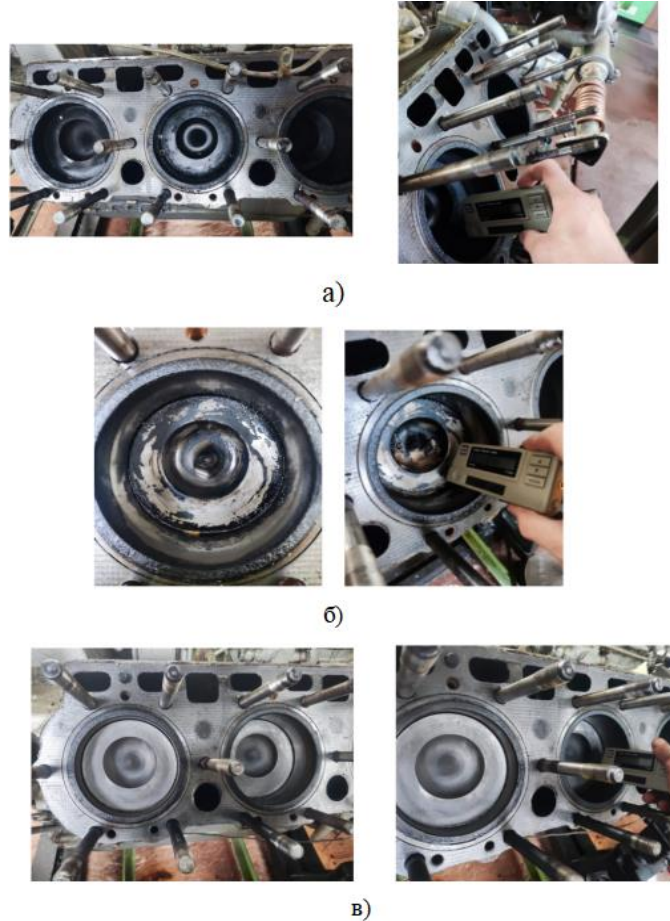
An analysis of the results of measuring the opacity of a diesel engine (YaMZ-236D-3) when operating on a conventional and ODT showed that there was a decrease in the opacity determined in units of the absorption coefficient (K) by almost 6%, and the opacity expressed in units of the attenuation coefficient (N) by almost 3%. The results obtained are due to the chemical activity of water contained in the ODT.

Thus, the developed device has demonstrated its operability, which allows us to conclude that the operation of the DEU on the ODT (with a water content of less than 5%) does not lead to a significant deterioration in the combustion dynamics of this fuel and it can be recommended for use on samples of the SHT. Next, the thickness of the carbon deposits on the DEU parts was assessed when operating on the ODT by partially disassembling it associated with removing the cylinder head and measuring the thickness of the carbon deposits before and after using the ODT. The appearance of the process of partial disassembly of the DEU (YaMZ-236D-3) is shown in Figure 10.



Figure 10.
External view of the process of partial disassembly of the DEU (YaMZ-236D-3).

After this the thickness of the carbon deposits was measured, which is shown in Figure 11.



a) before using the ODT; b) after 1.5 hours of operation of the DEU on the ODT; c) after 3 hours of operation of the DEU on the ODT.

Figure 11.

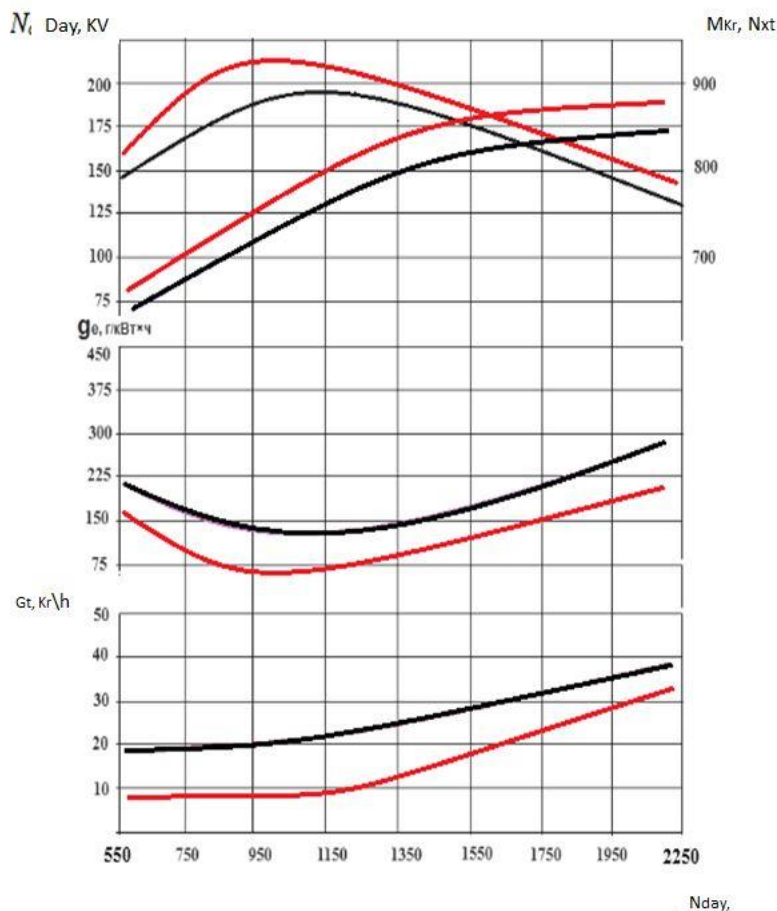
External appearance of pistons and measurement of the thickness of carbon deposits.

The results of measurements of the thickness of carbon deposits are presented in Table 2.

Table 2.
Results of measurements of the thickness of carbon deposits.

№ п/п	Operation designation	Average thickness of carbon deposits on the piston bottom, mm
1	Before using ODT	1,72
2	After 1.5 hours of DEU operation on ODT	0,24
3	After 3.0 hours of DEU operation on ODT	is completely absent

The obtained results allow us to conclude that after 3 hours of operation of the DEU on the ODT, its parts were completely cleaned of carbon deposits. Then, the external speed characteristics of the bench DEU (after 3 hours of operation of the DEU on the ODT) were determined, which are presented in Figure 12.



- curves obtained after 3 hours of operation of the DEU on the ODT;
- curves obtained before using the ODT

Figure 12.

External speed characteristic of the DEU (YaMZ-236D-3).

A comparative analysis of the graphical dependencies (curves) presented in Figure 12 shows that when the DEU operates on the ODT with the addition of a small amount of water (up to 5%) supplied to the combustion chamber after 3 hours of operation, the power of the DEU increased to 16%, the specific effective fuel consumption decreased to 18%.

3. Conclusions

the introduction of the developed technical device for the preparation of the ODT had a positive effect on the operation of the DEU, since all indicators improved, that is, the piston rings were decarbonized as a result of the complete cleaning of the crank mechanism and timing belt parts from carbon deposits. Consequently,, the developed device has shown its performance; the operation of a diesel engine on an ODT (with a water content of less than 5%) does not lead to a significant deterioration in the dynamics of the combustion process of this fuel and it can be recommended for use on SHT samples.

Acknowledgments:

The authors express their gratitude to the staff of the Department of Plant Protection, Faculty of Agricultural Engineering Sciences, Misan University, Tambov State Technical University and Megorinsk University.

Copyright:

© 2024 by the authors. This article is an open access article distributed under the terms and conditions of the Creative Commons Attribution (CC BY) license (<https://creativecommons.org/licenses/by/4.0/>).

References

- [1] Lomovskikh A.E. The influence of fuel emulsions on the environmental and ecological characteristics of internal combustion engines / Ivanov V.P., Illarionov V.V., Kapustin D.E. // Vestnik VAIU, issue No. 4 (11), 2010. pp. 159–164.
- [2] Svistula A.E. Increasing the performance of a diesel engine by improving mixture formation and combustion: abstract of thesis. dis. doctor. tech. Sci. Barnaul, 2007. 35 p.
- [3] Lozhkin V.N., Pimenov Yu.A., Safiullin R.N., Akodes A.A. Improving the environmental performance of automobile diesel engines by using water-fuel emulsions // Materials of a scientific-practical conference, 2005. 67–76 p.
- [4] Akulov N.I. Development of processes for producing emulsions of water-alcohol solutions in gasoline in rotary devices with flow modulation and their coagulation. M.: Nauka, 2005. 202 p.
- [5] Vlasov P.A., Skarlykin A.N. The influence of watered fuel on the technical condition of plunger pairs // Problems of development of machine technologies and technical means for the production of agricultural products: Collection of scientific proceedings. NPK dedicated to the 50th anniversary of the Faculty of Engineering of the Penza State Agricultural Academy. Penza: RIO PGSHA, 2002. pp. 77–80.
- [6] Rotary pulsation apparatus: Pat. 2190462 of the Russian Federation, IPC B01 F7/28. Ivanets V.N., Ivanets G.E., Afanasyeva M.M., Safonova E.A., Artemasov V.V.; applicant and patent holder Kemerovo Technological Institute of Food Industry. No. 2000128253/12; application 11/13/2000; publ. 10.10.2002. 4 s.
- [7] Rotary pulsation apparatus: Pat. 205615 Russian Federation, IPC B01 F7/28. Bogdanov V.V. [RU], Britov V.P. [RU], Kim V.V. Artemasov V.V. [UZ], Klotsung B.A. [RU], Smirnov B.L. [RU], Shkurin K.A. [RU]; applicant and patent holder St. Petersburg Institute of Technology. No. 5043511/26; application 05/22/1992; publ. 03/20/1996. 7 p.
- [8] Bigler V.I., Yudaev V.F., Danilychev O.I. Model of crushing a drop of natural emulsion in an unsteady flow of a hydrodynamic siren. M.: Mechanical Engineering, No. 1-2, 1997. 11 p.
- [9] Ivanets G.E., Plotnikov V.A., Plotnikov P.V. Energy characteristics of a rotary pulsation apparatus // Journal of Applied Chemistry. 2000. T. 73. No. 9. pp. 1511–1514.
- [10] Promtov M.A. Rotary pulsation devices: theory and practice: monograph. M.: Mashinostroenie-1, 2001. 260 p.
- [11] Dunaev, A.V., Al-Maidi, A.A.H., Rodionov, Y.V., Lomovskikh. Unique in composition and stability of water-fuel emulsion (2020) Journal of Advanced Research in Dynamical and Control Systems, 12 (4 Special Issue), pp. 432–439.
- [12] Al-Maidi, A.A.H., Rodionov, Y.V., Shchegolkov, A.V., Nikitin, D.V., Chernetsov, D.A., Mikheev, N.V. Mathematical modeling of thermo-regulation of fuel in diesel engines YaMZ-238 (YaMZ-238) (2018) Iraqi Journal of Agricultural Sciences, 49 (4), pp. 670–676.
- [13] Lomovskikh A.E. Preparation of fuel emulsions for internal combustion engines of military equipment based on a rotary pulsation apparatus / Ivanov V.P., Illarionov V.V., Tatarinov V.V. // Journal “Knowledge-Intensive Technologies”, No. 3, 2012. P.65–68.
- [14] Dolinsky A.A., Ivanitsky G.K. Principles for the development of new energy-saving technologies and equipment based on discrete-pulse energy input methods. Industrial. Thermal engineering. T.19. No. 4–5. 1997. pp. 13–25.
- [15] Chervyakov V.M., Koptev A.A. Determination of energy consumption in rotary devices // Chemical and oil and gas engineering. 2005. No. 4. pp. 10–12.
- [16] Buklagina G.V. Experience in modernizing MTZ tractors in Batoryevskaya agricultural machinery of the Chuvash Republic [Text] / Buklagina G.V. // Engineering and technical support of the agro-industrial complex: abstract journal, 2002. No. 2. P. 391.
- [17] Nikishina Yu.G. Development of devices to improve the environmental situation when using liquid hydrocarbon fuels. Kazan: Nauka, 2004. 154 p.
- [18] Aletdinova, Anna. (2016). Innovative development of the agro-industrial complex on the basis of disruptive technologies. St. Petersburg State Polytechnical University Journal. Economics. 251. 47-56. 10.5862/JE.251.5. DOI: 10.5862/JE.251.5
- [19] Gusev, A.. (2021). Material and technical base of the agro-industrial complex: trends and prospects on the way of innovation-oriented development. E3S Web of Conferences. 254. 10008. 10.1051/e3sconf/202125410008. DOI:10.1051/e3sconf/202125410008.
- [20] Altin, Orhan & Eser, Semih. (2004). Carbon deposit formation from thermal stressing of petroleum fuels. Am. Chem. Soc. Div. Fuel Chem.. 49. https://www.researchgate.net/publication/267420915_Carbon_deposit_formation_from_thermal_stressing_of_petro_oleum_fuels.